Catal Lett (2008) 125:1–7
DOI 10.1007/s10562-008-9539-9

Redox Isotherms for Vanadia Supported on Zirconia

Parag R. Shah · John M. Vohs · Raymond J. Gorte

Received: 7 May 2008 / Accepted: 3 June 2008 / Published online: 24 June 2008

Abstract Redox isotherms were measured for zirconia-supported vanadia between 10^{-2} and 10^{-28} atm at 748 K for two vanadia loadings, 2.9 and 5.8 V/nm^2, corresponding to isolated VO_4 species and monolayer, polymeric vanadates. The catalyst with isolated VO_4 species, which is expected to have predominantly V–O–Zr linkages, had a redox isotherm that showed a well-defined step corresponding to one oxygen per V. By contrast, the redox isotherm for the catalyst with polymeric vanadates changed more gradually with P_{O_2} and the change in the oxygen stoichiometry corresponded to 0.85 O/V. Comparison of these results to the redox isotherms for bulk vanadates suggests that oxidation of the isolated vanadates proceeds by a direct transition from $V^{+3} \leftrightarrow V^{+5}$, while transitions from $V^{+3} \leftrightarrow V^{+4}$ and $V^{+4} \leftrightarrow V^{+5}$ are possible with the polyvanadates. Rate measurements for methanol and propane oxidation over the two supported vanadia catalysts and several bulk vanadates showed that specific rates for each reaction were similar on all of the samples, suggesting that that the V–O bond strength does not affect the rate determining step of these reactions.

Keywords Supported catalyst · Vanadia · Vanadium oxide · Cerium vanadate · Magnesium vanadate · Zirconium vanadate · Zirconia · Coulometric Titration · Methanol oxidation · Formaldehyde · Oxidation · Redox · Equilibrium · Partial oxidation

---

P. R. Shah · J. M. Vohs · R. J. Gorte (✉)
Department of Chemical & Biomolecular Engineering,
University of Pennsylvania, Philadelphia, PA 19104, USA
e-mail: gorte@seas.upenn.edu

1 Introduction

Vanadia-based catalysts are used for a number of partial oxidation reactions including the oxidation of methanol to formaldehyde [1–4], the oxidation of *o*-xylene to phthalic anhydride [5, 6], and the oxidative dehydrogenation (ODH) of propane [7–9] and butane [10, 11] to produce alkenes. An important aspect of these catalysts is that the active form generally consists of highly dispersed vanadia supported on a second high-surface-area oxide such as TiO_2, ZrO_2, or Al_2O_3 [12]. As shown in Fig. 1, the vanadia can either be present in the form of isolated VO_4 species which have a tetrahedral geometry containing a single V=O bond and three V–O–S bonds (S = support cation), or polyvanadates that contain V–O–V bonds in addition to the V=O and V–O–S bonds [12, 13].

Since the oxidation reactions mentioned above are generally thought to proceed via a Mars-van Krevelen mechanism in which oxygen is removed and inserted into the oxide lattice, the redox properties of the catalyst are important and may affect catalytic properties. Indeed, the identity of the support has been reported to have a large effect on reactivity [2, 14], suggesting that the V–O–S bonds may play a role in the reactions. There are many studies in the literature in which the redox properties of supported vanadia and bulk vanadates have been characterized using temperature programmed oxidation and reduction (TPO and TPR) [2, 15–19]. While TPO/TPR measurements provide qualitative insights into the redox properties of oxides, quantitative measures, such as ΔG and ΔH of oxidation and reduction, cannot be determined using these techniques. In an effort to provide more quantitative data on the redox properties of vanadia catalysts and to determine how the local bonding in the lattice affects these properties, we have been using coulometric titration to

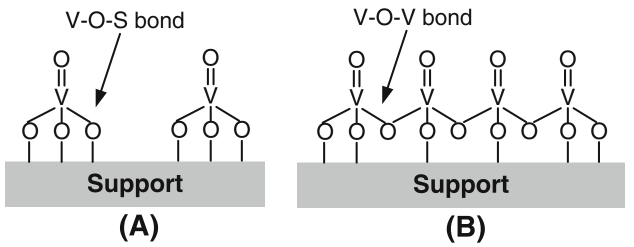

Fig. 1 Structures of supported vanadia: (**a**) isolated VO4 (**b**) polymeric VOX

measure redox isotherms, which are simply the equilibrium oxygen compositions of a sample as a function of the oxygen fugacity (P_{O_2}) at constant temperature, for bulk vanadates. Because the equilibrium constant for oxidation of a solid is related to P_{O_2}, the redox isotherms provide ΔG values for the oxidation reaction, and if data is collected at multiple temperatures, ΔH and ΔS can also be extracted.

In our previous studies we have reported the ΔG, ΔH, and ΔS values associated with the oxidation and reduction of V_2O_5, $Mg_3(VO_4)_2$, $CeVO_4$ and ZrV_2O_7, and ΔG values for $AlVO_4$, $LaVO_4$, $CrVO_4$ [20, 21]. As will be discussed in more detail below, for these materials only the vanadium ions undergo redox and these reactions are strongly influenced by the local bonding and the identity of the other cation in the mixed oxide. In the present study we have extended this work to include quantification of the redox properties of supported vanadia catalysts. Redox isotherms for both isolated vanadate and polyvanadate species supported on ZrO_2 were measured at 748 K and ΔG for the redox reactions are reported. The rates for the oxidation of methanol and propane on several bulk vanadates and the supported vanadia catalysts are also reported in order to allow the influence of the redox properties on reactivity to be assessed.

2 Experimental

2.1 Catalyst Preparation and Characterization

Vanadia was deposited on the ZrO_2 support (synthesized by decomposing $ZrO(NO_3)_2$ in air, 57 m^2/g) by wet impregnation of a solution of ammonium metavanadate (NH_4VO_3, Sigma) and oxalic acid ($C_2H_2O_4$, Aldrich). After drying in air at 400 K the samples were ground with a mortar and pestle and calcined at 758 K in air for 4 h. Supported samples with vanadia weight loadings of 2.5% (2.5VZr), 5% (5VZr) and 10% (10VZr) were prepared.

ZrV_2O_7 was synthesized by evaporating an aqueous solution of $ZrO(NO_3)_2$ and ammonium metavanadate (1:2 molar ratio), and oxalic acid. The dried precipitate was ground with a mortar and pestle and calcined in air at 973 K for 24 h. $CeVO_4$ was prepared in a similar manner, using $Ce(NO_3)_3$ as the Ce precursor and calcining in air it at 1,073 K for 24 h. $Mg_3(VO_4)_2$ was prepared using $Mg(NO_3)_2$ as the precursor and citric acid instead of oxalic acid and calcining in air at 973 K for 6 h. The bulk V_2O_5 (99.99%) was obtained from Aldrich and was calcined in air at 898 K for 2 days prior to use.

Raman spectra were obtained at room temperature under ambient conditions using a Renishaw RM1000 VIS Raman Microspectrometer with 514.5 nm Ar laser as the excitation source. XRD patterns for the bulk vanadates were collected using a Rigaku Geigerflex diffractometer with a Cu(Kα) radiation source ($\lambda = 1.5405$ Å). The surface areas for all catalysts were determined using the BET method using N_2.

2.2 Measurement of Redox Isotherms

Coulometric titration was used to measure redox isotherms, the sample composition as a function of the P_{O_2} at constant temperature, of the supported vanadia catalysts and the bulk vanadates. A detailed description of the coulometric titration cell and apparatus has been reported previously [21–25] and only a brief description will be given here. Approximately 0.4 g of sample was loaded into a yttria stabilized zirconia (YSZ) tube, which was sealed at one end by an O_2 sensor consisting of a dense YSZ wafer with porous Ag electrodes on both its inner and outer surfaces. A thin layer of mixed ceria-zirconia was also placed between the Ag electrode and the YSZ wafer on the inner (sample) side to improve its performance for oxygen pumping. The tube was then placed in a furnace and heated to 748 K. For measurements starting from the oxidized state of the sample, a mixture of 4.5% O_2, 9.5% CO_2 and 86% Ar, corresponding to a P_{O_2} of 4.5×10^{-2} atm., was then flowed over the sample for 1 h, after which the tube was sealed and the sample was allowed to equilibrate with the gas phase. For measurements starting from the reduced state of the sample, the sample was reduced either by flowing 10% CO in He, or by electrochemically pumping out O_2 after the abovementioned O_2/Ar/CO_2 gas mixture was flowed over the sample and the tube sealed. The P_{O_2} in the cell was determined from the voltage across the YSZ disk, using the Nernst equation. Controlled amounts of O_2 could be pumped in and out of the cell by the application of a potential across the YSZ electrolyte using a Gamry Instruments potentiostat with 1 C of charge corresponding to to 2.6 μmol O_2. After each O_2 pumping step, the sample was allowed to equilibrate from 3 to 15 days. It was assumed that the sample and gas phase had equilibrated when the sensor voltage changed by less than 0.3 mV/h.

2.3 Reaction Studies

Rates for the selective oxidation of methanol over the various catalysts were measured using a micro-flow reactor equipped with an on-line gas chromatograph (SRI-8610C) with a TCD detector. When measuring the methanol oxidation rates for the bulk vanadates, an amount of catalyst containing 0.7 m^2 of surface area was used. For comparing rates over supported vanadia and bulk vanadia, the catalyst loading was equivalent to 5×10^{18} vanadium atoms and 1.25×10^{19} vanadium atoms for methanol and propane oxidation reactions respectively. Methanol oxidation rates were measured by passing a gas containing He, O_2, and CH_3OH in a 22.5:2:1 molar ratio, while the He:O_2:C_3H_8 molar ratio was 17.6:1.57:1 for propane oxidation measurements. A total flow rate of 100 cm^3/min was maintained for both reactions. The propane oxidation study over supported vanadates was performed at temperatures lower than 773 K to prevent reaction of vanadia with ZrO_2. The conversion was less than 20% in all cases, so that differential reaction conditions could be assumed.

3 Results and Discussion

3.1 Catalyst Characterization

Characterization data for the bulk vanadates has been discussed in a previous paper. X-ray diffraction patterns each of these samples showed that they were single phase. The BET surface areas of the bulk vanadates are reported in Table 1. The surface areas were very low because of the prolonged sintering times required for forming a single-phase material. The surface areas of the supported catalysts, along with the vanadium surface densities, are reported in Table 2 and are more typical of catalytic materials. Figure 2a displays Raman spectra of the supported vanadia samples and the ZrO_2 support under ambient conditions between 200–1,100 cm^{-1}. An expanded view of the 700–1,100 cm^{-1} region of the spectra is shown in Fig. 2b. The peaks between 200 and 700 cm^{-1} in the spectrum of the support (spectrum a) are characteristic of the monoclinic phase of ZrO_2 [26]. The support does not have any intense peaks between 700 and 1,100 cm^{-1}. In addition to the peaks characteristic of the ZrO_2, the Raman spectrum of the 2.5ZrV sample (spectrum b) contains a peak centered at 988 cm^{-1} which can be attributed to the V=O stretch of surface vanadate species [27, 28]. Broad overlapping features are also evident between 700 and 950 cm^{-1}. These features have previously been attributed to overlapping bands associated with both V=O and V–O–V vibrations in polyvanadates [27]. The intensities of the ZrO_2 bands for the ZrV2.5 sample are the same as that for the bare support, implying that significant portions of the ZrO_2 surface are still exposed.

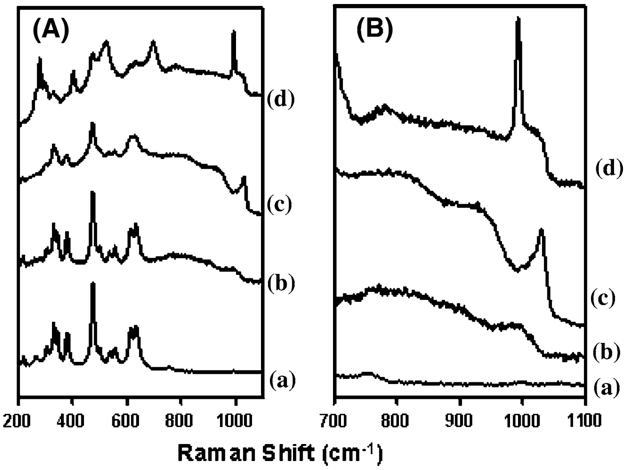

Fig. 2 Raman Spectra of (a) ZrO_2, (b) 2.5 wt.% V_2O_5 on ZrO_2, (c) 5wt.% V_2O_5 on ZrO_2, (d) 10wt.% V_2O_5 on ZrO_2

Table 1 Surface areas of bulk vanadates

Sample	Surface area (m^2/g)
V_2O_5	1.35
ZrV_2O_7	0.27
$CeVO_4$	0.85
$Mg_3(VO_4)_2$	5.0

The spectrum for the 5ZrV sample (spectrum c) shows an increase in the intensity of the features associated with the vanadia. The position of the V=O stretching mode also shifted up in energy to 1,028 cm^{-1}. Based on previous studies, the changes in the spectra with increasing vanadia loading can be attributed to a shift from isolated vanadates in the 2.5ZrV sample to polyvanadates in the 5ZrV sample [26–28]. Thus, the 2.5ZrV sample contains predominantly isolated VO_4 species with V=O and V–O–Zr bonds, while the 5ZrV sample contains predominantly polyvanadates with V=O, V–O–Zr, and V–O–V bonds. The vanadia coverage in the 5ZrV sample is 5.8 V/nm^2, which is a little

Table 2 Surface areas of supported vanadates

Sample	Vanadia loading (weight %)	Vanadium surface density (V/nm^2)	Sample area (m^2/g)
2.5ZrV	2.5	2.9	57
5ZrV	5	5.8	43
10ZrV	10	11.6	–

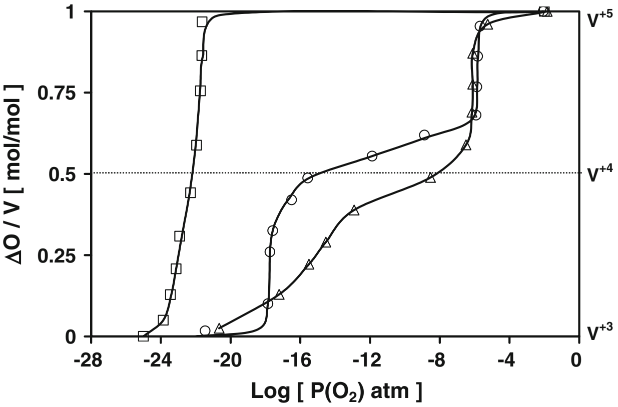

Fig. 3 Redox isotherms at 873 K for (□) $CeVO_4$, (○) V_2O_5, and (Δ) ZrV_2O_7

less than the reported monolayer coverage on ZrO_2 of 7 V/nm^2 [27].

More dramatic changes in the Raman spectrum were observed for the 10ZrV sample (spectrum d) including the appearance of a sharp peak at 995 cm^{-1} which is characteristic of the V=O stretch in bulk V_2O_5 [26]. The emergence of peaks at 991, 693, 520, 400, 280 cm^{-1}, is also consistent with the formation of V_2O_5 [26]. This is the expected result since the vanadia coverage for this sample, 11.6 V/nm^2, is well above that required for a monolayer.

3.2 Redox Isotherms

As noted earlier, we have previously shown that the nature of the local bonding in bulk vanadates significantly affects their redox properties [20, 21]. For comparison purposes it is useful to consider the redox isotherms for several bulk vanadates before presenting the data for the supported vanadia samples. Figure 3 displays equilibrium isotherms for $CeVO_4$, V_2O_5, and ZrV_2O_7 at 873 K. For all three oxides, the change in oxygen stoichiometry going from low to high P_{O_2} corresponds to exactly one oxygen per V atom. For $CeVO_4$, this change in oxygen stoichiometry occurs in a single step at a P_{O_2} of 5×10^{-23} atm, with bulk composition changing from $CeVO_3$ to $CeVO_4$. This isotherm can be understood by considering the zircon structure of $CeVO_4$ in which all the oxygens are equivalent and bridge between Ce^{+3} and V^{+5} ions (i.e. Ce–O–V) [29]. Since +3 is the lowest stable oxidation state for Ce (except for the metal), removal of an oxygen atom from the lattice results in reduction of the neighboring vanadium cation from V^{+5} to V^{+3}. Therefore, the step in the isotherm from $CeVO_3$ to $CeVO_4$ corresponds to a $V^{+5} \leftrightarrow V^{+3}$ transition.

In contrast to $CeVO_4$, the isotherm for V_2O_5 at 873 K exhibits two steps at P_{O_2} values of 2×10^{-18} and 1×10^{-6} atm. All the oxygens in the layered structure of V_2O_5 are not equivalent and this material contains both V–O–V and V=O bonds [29]. Removal of a bridging oxygen atom results in reduction of each of the neighboring vanadium cations from V^{+5} to V^{+4}. Thus, this material can undergo stepwise reduction from V_2O_5 to VO_2 to V_2O_3 and the two steps in the isotherm can be attributed to $V^{+5} \leftrightarrow V^{+4}$ ($P_{O_2} = 1 \times 10^{-6}$ atm) and $V^{+4} \leftrightarrow V^{+3}$ ($P_{O_2} = 2 \times 10^{-18}$) transitions. Because oxides with mixed valencies exist at intermediate oxidation states, the transition between the two steps is gradual. The isotherm for ZrV_2O_7 is similar to that for V_2O_5, although the transition at lower P_{O_2} is less sharp. Zirconium vanadate has a complex structure [30] that contains both Zr–O–V and V–O–V bonds. Only the vanadium cations would be expected to undergo oxidation and reduction and the two transitions in the isotherm can again be assigned to $V^{+5} \leftrightarrow V^{+4}$ and $V^{+4} \leftrightarrow V^{+3}$.

Figure 4 shows the redox isotherm for the 2.5ZrV sample obtained by coulometric titration. The measurements for this catalyst were performed twice on two samples from the same batch. In the first experiment, the titration was started with a fully oxidized sample (open circles) and the composition was measured for P_{O_2} values decreasing from 10^{-1} to 10^{-28} atm, the point at which the sample was completely reduced to V^{+3}. To test for reversibility, the isotherm was then re-measured on a second sample from the same batch of catalyst, starting with the fully reduced sample (black circles). The results were identical, demonstrating the expected reversibility for equilibrium measurements. The change in oxygen stoichiometry going from low to high P_{O_2} correspond to approximately one oxygen per V, which is again very close to the stoichiometry observed for the bulk vanadates. The shape of the isotherm is similar to that observed with $CeVO_4$, with the oxygen stoichiometry changing in a single, somewhat broad, step centered at a P_{O_2} of 1×10^{-21} atm. By analogy to $CeVO_4$, the step can be assigned to a $V^{+5} \leftrightarrow V^{+3}$ transition.

The lack of stable species containing V^{+4} in the redox isotherm for 2.5ZrV can be understood if one considers the structure of the isolated vanadate species in this sample (see Fig. 1). Since the Zr^{+4} ions in the support cannot be reduced, removal of an oxygen atom from the vanadate results in reduction of the V^{+5} to V^{+3}. There are two choices, however, as to which oxygen is removed, the bridging V–O–Zr or the terminal V=O. It seems unlikely that it would be the latter, since this is the more strongly bound of the two based on vibrational frequencies. The conclusion that the bridging oxygen is removed is also supported by comparison of the Gibbs free energies of reduction for the 2.5ZrV sample with that for the bulk vanadates, $CeVO_4$ and $Mg_3(VO_4)_2$, which contain only M–O–V bridging oxygens. The ΔG of reduction for these compounds are listed in Table 3 along with the value for the 2.5ZrV sample determined from the data in Fig. 4.

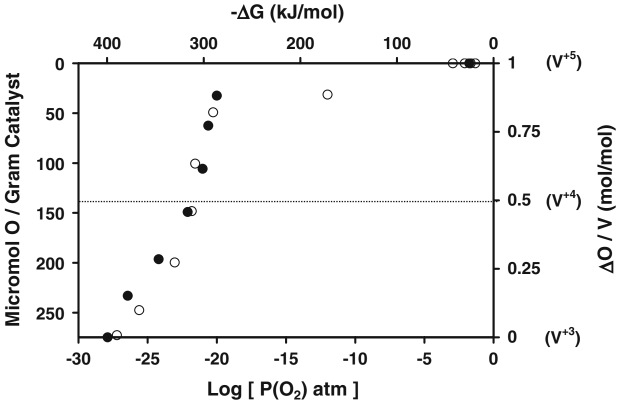

Fig. 4 Redox isotherm for 2.5wt.% V_2O_5 on ZrO_2 at 748 K. Open circles are for a run starting with a fully oxidized sample and the closed circles are for run starting with a reduced sample

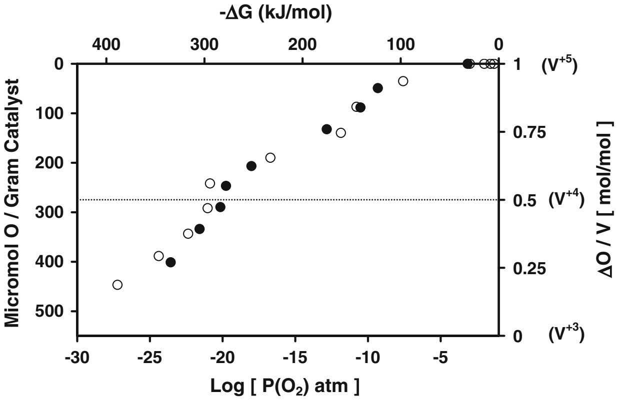

Fig. 5 Redox isotherm for 5wt.% V_2O_5 on ZrO_2 at 748 K. Open circles are for run starting with a an oxidized sample, and the closed circles are for run starting with a reduced sample

Notice that the ΔG values for the bulk vanadates were measured at 873 K and have been extrapolated to 748 K by assuming ΔH is independent of temperature in order to facilitate comparison with the lower temperature data collected here. Data from bulk oxides with M–O–V bridging oxygens also indicated that ΔG decreases with increasing Pauling electronegativity of the M cation [21]. The electronegativity values are also listed in the Table. Extending the electronegativity correlation to the 2.5ZrV sample, the data in Table 3 suggest that ΔG for 2.5ZrV (−300 kJ/mol) should be close to that for $Mg_3(VO_4)_2$ (−287 kJ/mol) which is indeed the case. This result provides further support for the conclusion that reduction of the isolated vanadates in the 2.5ZrV sample proceeds via removal of one of the oxygens that bridges between the vanadium cation and the support.

The isotherms for 5ZrV sample shown in Fig. 5 were measured starting from the fully oxidized state and the reduced state, with two different samples from the same batch. The isotherms are identical, which implies that the measurements are reversible. In contrast to the 2.5ZrV sample, the isotherm for 5ZrV does not contain a single step corresponding to a $V^{+5} \leftrightarrow V^{+3}$ transition but is more complex with the equilibrium O/V ratio, decreasing continually as the P_{O_2} is decreased from 10^{-6} to 10^{-28} atm. As discussed earlier, the 5ZrV sample is composed of polyvanadates that contain both V–O–V and V–O–Zr bonds. By analogy to ZrV_2O_7, which has similar oxygen coordinations, both $V^{+5} \leftrightarrow V^{+4}$ and $V^{+4} \leftrightarrow V^{+3}$ transitions would be expected to occur. This indeed appears to be the case and reduction takes place over the entire pressure range observed for ZrV_2O_7. The lack of sharp steps in the isotherm for 5ZrV can be attributed to the heterogeneous nature of this sample, since it is likely to contain polyvanadates with a distribution of clusters sizes as well as some isolated species.

Table 3 Pauling electronegativities and ΔG of oxidation

M atom	Pauling electronegativity of M atom	ΔG (kJ/mol)
$CeVO_4$ (Ce–O–V bond)	1.1	−392
$Mg_3(VO_4)_2$ (Mg–O–V bond)	1.31	−287
2.5ZrV (Zr–O–V bond)	1.33	−300

Another interesting aspect of the redox isotherm for the 5ZrV sample is that the change in oxygen stoichiometry going from high to low P_{O_2} corresponds to reduction of only 85% of the cations to V^{+3}, assuming that all of the V was initially in the +5 oxidation state. Complete reduction of all the vanadium cations to V^{+3} did not occur for P_{O_2} values as low as 10^{-28} atm. We believe it is unlikely that this discrepancy is due to experimental uncertainties, since complete reduction to V^{+3} was observed for the 2.5ZrV sample. The result is consistent, however, with several other studies in the literature where the amount of O_2 removed from supported vanadia samples was quantified using temperature-programmed reduction (TPR) [31–34]. Those studies reported that between 10 and 40% of the vanadium cations could not be reduced to V^{+3}. One possible explanation for this result is that removal of the V–O–V bridging oxygen at the end of a polyvanadate chain produces an isolated VO_3 group containing a V^{+4} cation. Since the Zr^{+4} cations of the support are essentially non-reducible, further reduction of the VO_3 species would require the formation of V^{+2}, which requires a much lower P_{O_2} than that obtainable in our apparatus.

The redox isotherms obtained in this study demonstrate dramatic differences in the thermodynamic properties of isolated and polyvanadates supported on ZrO_2. ΔH values for the redox reactions of the supported vanadia were not obtained in the present study, since data was collected at only one temperature. Nonetheless, the shapes of the redox isotherms clearly indicate that the polyvanadates are much more easily reduced than the isolated vanadates. For the polyvanadates at 748 K the onset of reduction of V^{+5} to V^{+4} occurs at a P_{O_2} of $\sim 10^{-6}$ atm and deeper reduction to V^{+3} occurs below 10^{-20} atm. In contrast, the onset of reduction of the isolated vanadates at 748 K occurs at a P_{O_2} of 10^{-20} atm where a one step reduction from V^{+5} to V^{+3} occurs.

Variations in the catalytic activity are one possible consequence of the differences in the redox properties of the isolated and polyvanadates. Indeed, there are several reports in the literature where turnover frequencies on supported vanadia catalysts have been found to be a function of the vanadia coverage [7, 35–37]. In order to further investigate this possibility, the reactivity of the 2.5ZrV and 5ZrV samples was measured along with the reactivity of several bulk vanadates for the selective oxidation of methanol and the oxidative dehydrogenation (ODH) of propane. For the bulk vanadates, the reaction rates have been normalized per unit area, whereas the rates for the supported vanadia samples have been normalized per vanadium atom and reported as turnover frequencies (TOF). For comparing reaction rates on bulk and supported vanadia samples, the surface density of vanadium ions in the bulk V_2O_5 was assumed to be 7 V/nm^2.

Rates for the selective oxidation of methanol on bulk and supported vanadates are reported in Fig. 6a, b, respectively. The selectivity to formaldehyde was greater than 90% for all catalysts. As shown in Fig. 6a, the rate of consumption of methanol was similar on all of the bulk vanadates, with the exception of $Mg_3(VO_4)_2$ which exhibited specific rates $\sim$3 times less than the other oxides. Figure 6b shows that the TOF for the 2.5ZrV and 5ZrV samples were also similar and close to that for bulk vanadia. The activation energies for all catalysts are between 70–85 kJ/mol, which are consistent with values reported in the literature [2, 14].

Figure 7 shows the TOF for propane consumption during ODH on bulk vanadia, and the 2.5ZrV and 5ZrV supported vanadia samples. For the temperature range studied, the propane conversion varied from 4–10%. Only very small variations in the TOF were observed for the two supported vanadia samples and these samples exhibited slightly higher TOF than bulk V_2O_5. The selectivity to propene was similar for the supported vanadates decreasing from 65% to 45% with increasing temperature. The propene selectivity for bulk V_2O_5 was slightly lower than that for the supported vanadates. The activation energy for propane consumption over these catalysts ranged between 65–72 kJ/mol which is similar to those reported in literature [9].

The thermodynamic data obtained by coulomb titration indicate that for the bulk vanadates, the binding of oxygen atoms in the lattice‘ decreases in the order $CeVO_4 > Mg_3(VO_4)_2 > V_2O_5 \approx ZrV_2O_7$. In light of this and the differences in the redox isotherms for these materials, it is surprising that the rates for the selective oxidation of methanol are nearly identical for $CeVO_4$, V_2O_5 and ZrV_2O_7, with the rate on $Mg_3(VO_4)_2$ being only slightly lower. While differences in surface and bulk properties is one possible explanation for the lack of correlation between catalytic activity and the bulk redox isotherms, this result is consistent with that reported recently by Routray et al. [38] who observed that the rate of methanol oxidation on bulk vanadates does not correlate with the V–O bond strengths determined from vibrational frequencies in Raman spectra. Together, these results suggest that breaking of V–O bonds does not occur in the rate determining step for methanol oxidation on these materials.

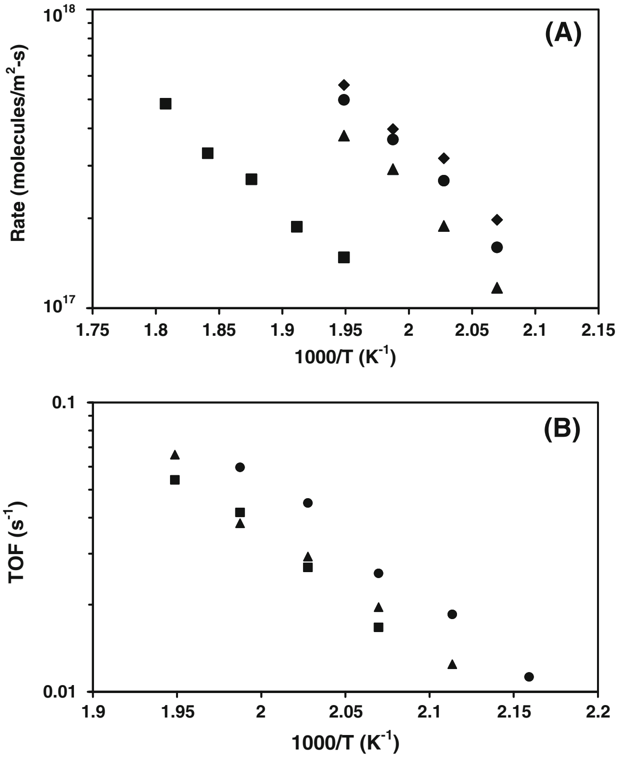

Fig. 6 (**a**) Rate of methanol oxidation on (▲) V_2O_5, (●) ZrV_2O_7, (◆) $CeVO_4$, and (■) $Mg_3(VO_4)_2$. (**b**) Turnover frequencies for methanol oxidation on (■) V_2O_5, (●) 2.5 wt.% V_2O_5 on ZrO_2, and (▲) 5wt. % V_2O_5 on ZrO_2. All rates were collected with a gas stream consisting of $He:O_2:CH_3OH = 22.5:2:1$ molar ratios with a total flow rate of 100 cm^3/min

The results of the present study lead to a similar conclusion for supported vanadia. In spite of the dramatic differences in the redox isotherms for the 2.5ZrV and 5ZrV samples, which showed that the supported polyvanadates are much easier to reduce than the isolated vanadates, the TOF per vanadium cation for methanol oxidation on these catalysts were nearly identical, both to themselves and to

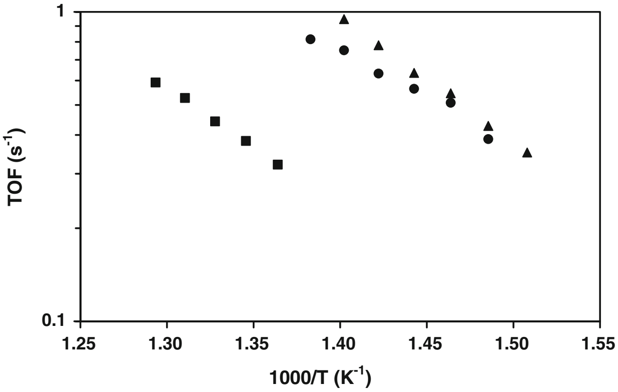

Fig. 7 Turnover frequencies for propane oxidation on (■) V_2O_5, (●) 2.5 wt.% V_2O_5 on ZrO_2, and (▲) 5wt. % V_2O_5 on ZrO_2. All rates were collected with a gas stream consisting of $He{:}O_2{:}C_3H_8 = 17.6{:}1.57{:}1$ molar ratios with a total flow rate of 100 cm^3/min

the bulk oxides. This was also the case for the ODH of propane on the supported vanadia catalysts and bulk V_2O_5. For the supported vanadia samples, there is no confusion as to whether the redox isotherms correspond to the active form of the vanadia in the catalyst. These results, therefore, again indicates that V–O bond scission is not rate limiting in these reactions.

4 Conclusions

Redox isotherms for vanadia supported on zirconia were determined as a function of vanadia loading. For the 2.5ZrV sample which contains predominantly isolated vanadates, reduction from V^{+5} to V^{+3} occurred in a single transition at a P_{O_2} of 1×10^{-20} atm at 748 K. Reduction of the 5VZr sample which contained predominantly poly-vanadates proceeded in a stepwise fashion, $V^{+5} \rightarrow V^{+4} \rightarrow V^{+3}$, over a wide P_{O_2} range (10^{-2}–10^{-28} atm) at 748 K. In spite of the differences in the redox properties of the supported vanadia catalysts exhibited similar activity for the selective oxidation of methanol and propane ODH suggesting that V–O bond scission is rate limiting for these reactions.

Acknowledgements The authors would like to acknowledge the Materials Characterization Facility at Drexel University for providing the Raman Spectrometer. This work was supported by the Department of Energy, Office of Basic Energy Sciences, Chemical Sciences, Geosciences and Biosciences Division, Grant DE-FG02-85ER13350.

References

1. Forzatti P, Tronconi E, Elmi AS, Busca G (1997) Appl Catal A 157:387
2. Deo G, Wachs IE (1994) J Catal 146:323
3. Briand LE, Jehng JM, Cornaglia L, Hirt AM, Wachs IE (2003) Catal Today 78:257
4. Feng T, Vohs JM (2004) J Catal 221:619
5. Dias CR, Portela MF (1997) Catal Rev Sci Engin 39:169
6. Spengler J, Anderle F, Bosch E, Grasselli RK, Pillep B, Behrens P, Lapina OB, Shubin AA, Eberle HJ, Knozinger H (2001) J Phys Chem B 105:10772
7. Khodakov A, Olthof B, Bell AT, Iglesia E (1999) J Catal 181:205
8. Pieck CL, Banares MA, Fierro JLG (2004) J Catal 224:1
9. Shee D, Rao TVM, Deo G (2006) Catal Today 118:288
10. Jackson SD, Rugmini S (2007) J Catal 251:59
11. Owens L, Kung HH (1994) J Catal 148:587
12. Weckhuysen BM, Keller DE (2003) Catal Today 78:25
13. Wachs IE, Weckhuysen BM (1997) Appl Catal A 157:67
14. Bronkema JL, Bell AT (2008) J Phys Chem C 112:6404
15. Chen KD, Xie SB, Bell AT, Iglesia E (2000) J Catal 195:244
16. Roozeboom F, Mittelmeijerhazeleger MC, Moulijn JA, Medema J, Debeer VHJ, Gellings PJ (1980) J Phys Chem 84:2783
17. Steinfeldt N, Muller D, Berndt H (2004) Appl Catal A 272:201
18. De M, Kunzru D (2004) Catal Lett 96:33
19. Ruitenbeek M, van Dillen AJ, de Groot FMF, Wachs IE, Geus JW, Koningsberger DC (2000) Top Catal 10:241
20. Shah PR, Vohs JM, Gorte RJ (2007) J Phys Chem B 111:5680
21. Shah PR, Khader MM, Vohs JM, Gorte RJ (2008) J Phys Chem C 112:2613
22. Shah PR, Kim T, Zhou G, Fornasiero P, Gorte RJ (2006) Chem Mater 18:5363
23. Zhou G, Shah PR, Montini T, Fornasiero P, Gorte RJ (2007) Surf Sci 601:2512
24. Zhou G, Shah PR, Gorte RJ (2008) Catal Lett 120:191
25. Zhou G, Shah PR, Kim T, Fornasiero P, Gorte RJ (2007) Catal Today 123:86
26. Gao X, Jehng J-M, Wachs IE (2002) J Catal 209:43
27. Su SC, Bell AT (1998) J Phys Chem B 102:7000
28. Deo G, Wachs IE (1991) J Phys Chem 95:5889
29. Da Silva JLF, Ganduglia-Pirovano MV, Sauer J (2007) Phys Rev B Condens Matter 76:125117
30. Evans JSO, Hanson JC, Sleight AW (1998) Acta Crystallogr Sect B Struct Sci 54:705
31. Adamski A, Sojka Z, Dyrek K, Che M, Wendt G, Albrecht S (1999) Langmuir 15:5733
32. Wu Z, Stair PC, Rugmini S, Jackson SD (2007) J Phys Chem C 111:16460
33. Frank K, Wolff T, Lorenz H, Seidel-Morgenstern A, Suchorski Y, Piorkowska M, Weiss H (2007) J Catal 247:176
34. Occhiuzzi M, Tuti S, Cordischi D, Dragone R, Indovina V (1996) J Chem Soc Faraday Trans 92:4337
35. Argyle MD, Chen KD, Bell AT, Iglesia E (2002) J Catal 208:139
36. Khodakov A, Yang J, Su S, Iglesia E, Bell AT (1998) J Catal 177:343
37. Chen KD, Khodakov A, Yang J, Bell AT, Iglesia E (1999) J Catal 186:325
38. Routray K, Briand LE, Wachs IE (2008) J Catal 256:145